

Research



Cite this article: Cayado P, Li M, Erbe M, Liu Z, Cai C, Hänisch J, Holzapfel B. 2020 REBCO mixtures with large difference in rare-earth ion size: superconducting properties of chemical solution deposition-grown $\text{Yb}_{1-x}\text{Sm}_x\text{Ba}_2\text{Cu}_3\text{O}_{7-\delta}$ films. *R. Soc. Open Sci.* **7**: 201257. <http://dx.doi.org/10.1098/rsos.201257>

Received: 27 July 2020

Accepted: 19 October 2020

Subject Category:

Chemistry

Subject Areas:

materials science

Keywords:

YbSmBCO , chemical solution deposition, extremely low fluorine, rare-earth ion size, pinning performance

Authors for correspondence:

Pablo Cayado

e-mail: pablo.cayado@kit.edu

Jens Hänisch

e-mail: jens.haenisch@kit.edu

This article has been edited by the Royal Society of Chemistry, including the commissioning, peer review process and editorial aspects up to the point of acceptance.

REBCO mixtures with large difference in rare-earth ion size: superconducting properties of chemical solution deposition-grown $\text{Yb}_{1-x}\text{Sm}_x\text{Ba}_2\text{Cu}_3\text{O}_{7-\delta}$ films

Pablo Cayado¹, Minjuan Li², Manuela Erbe¹,
Zhiyong Liu², Chuanbing Cai², Jens Hänisch¹
and Bernhard Holzapfel¹

¹Karlsruhe Institute of Technology (KIT), Institute for Technical Physics (ITEP), Hermann-von-Helmholtz-Platz 1, 76344 Eggenstein-Leopoldshafen, Germany

²Shanghai Key Laboratory of High Temperature Superconductors, Physics Department, Shanghai University, Shanghai 200444, People's Republic of China

PC, 0000-0003-3703-6122; JH, 0000-0003-2757-236X

The main objective of this work was to study the superconducting properties of REBCO films with a mixture of rare-earth (RE) ions with large difference in ion size, in particular Sm^{3+} and Yb^{3+} . These $\text{Yb}_{1-x}\text{Sm}_x\text{Ba}_2\text{Cu}_3\text{O}_{7-\delta}$ films have been successfully prepared for the first time by chemical solution deposition following the extremely low-fluorine route, which allows reducing the fluorine content by 93% with respect to standard full trifluoroacetate solutions. On the one hand, critical temperature T_c remains stable at approximately 90 K with Sm content up to $x = 0.5$ where T_c starts to increase towards the values of pure SmBCO films of approximately 95 K. On the other hand, the critical current densities J_c of the pure SmBCO films are the largest at 77 K, where the influence of a higher T_c is very relevant, while at lower temperatures and low fields, the mixed films reach larger values. This demonstrates that mixing rare-earth elements RE in $\text{REBa}_2\text{Cu}_3\text{O}_{7-\delta}$ causes a change in the pinning properties of the films and reveals the importance of selecting adequate REBCO compounds according to the temperature and magnetic field region of a desired application.

1. Introduction

In recent years, the second-generation (2G) high- T_c superconducting tapes, the coated conductors (CCs) have captured large interest in applied superconductivity [1–3]. Their high critical current densities, also in high magnetic fields, make them very attractive for numerous applications such as high-field magnets, motors, generators and fault-current limiters. However, in order to spread their use in those applications, the currently available CCs still require an improvement of their performance, i.e. the superconducting properties of the $REBa_2Cu_3O_{7-\delta}$ (REBCO) films within the CC's architecture need to be enhanced.

One of the options for achieving such improvements is the use of alternative REBCO compounds, i.e. compounds with rare-earth (RE) ions other than Y^{3+} , which forms $YBa_2Cu_3O_{7-\delta}$ (YBCO), the best-studied REBCO compound. For some of those alternative cases, improved superconducting properties compared to YBCO have been reported [4–8]. However, the synthesis of these compounds is occasionally more complicated than for YBCO. On the one hand, large RE ions, like Nd^{3+} or Sm^{3+} , tend to partially replace the Ba^{2+} ions and, on the other hand, small RE^{3+} ions, such as Yb^{3+} and Lu^{3+} , do not fit satisfactorily in their lattice site, generating vacancies. Both facts cause a drastic decrease in the REBCO phase stability and superconducting properties [9–11]. In particular, the syntheses of SmBCO and YbBCO films are probably two of the most challenging ones among the REBCO phases because the ion size of both compounds are almost at the superior and inferior ends of the line of possible lanthanide candidates. Recently, our group has been able to prepare SmBCO films by chemical route showing the difficulties associated with the tendency of Sm^{3+} ions to occupy the Ba^{2+} sites [12]. Also, several works reported the problems in preparing YbBCO films, leading, in general, to quite modest maximum critical temperatures $T_c \sim 90$ K and self-field critical current densities, J_c^{sf} , at 77 K of approximately 1 MA cm^{-2} [13–18].

Another approach, and probably the most important one, for improving the superconducting properties of REBCO films is to increase the flux pinning. Besides the usual strategy of preparing nanocomposites, e.g. by adding non-superconducting perovskite nanoparticles, several studies reported on possible flux pinning enhancement in RE mixture compositions with respect to the standard pure REBCO compounds [19–21]. The RE elements involved in these mixed compounds and their ratio have to be chosen wisely. The optimum crystallization temperatures of the different REBCO phases depend on the RE: they increase continuously from the REBCO compounds with smaller ions (YbBCO, ErBCO, YBCO) to those with bigger ions (EuBCO, SmBCO, NdBCO) reaching even more than 100°C of difference [22,23]. Therefore, the synthesis of mixed compounds with a large difference in RE ion size may be more difficult and require a compromise between two optimal temperatures that might be more than 100°C apart.

The chosen technique to prepare the films for this study is the low-cost, versatile and easy-to-scale chemical solution deposition (CSD). Most of the works using this technique are based on the well-known trifluoroacetate–metal organic decomposition (TFA-MOD) route [24], in which the fluorine-containing precursor solutions decompose in the pyrolysis to metal fluorides avoiding the undesirable formation of $BaCO_3$. This compound is very difficult to decompose in the subsequent crystallization stage since much larger temperatures would be needed than used in the crystallization process [25]. However, despite the advances in recent years, the TFA-MOD route still needs quite long times to obtain defect-free pyrolysed films [7,26–28], and to shorten this process would be desirable to increase the production rates.

The time restrictions associated with the pyrolysis in the TFA-MOD route can be overcome by changing the solution formulation towards lower contents of fluorinated precursors [29–31]. For YBCO films, Li *et al.* [32] recently tested several precursor solutions with different fluorine contents: the conventional low-fluorine solution with a fluorine content of 54%, the super low-fluorine solution with a fluorine content of 31% and the extremely low-fluorine (ELF) solution with a fluorine content of only 7% with respect to the full trifluoroacetates (TFA) solution. All these low-fluorine solutions still follow the so-called BaF_2 reaction mechanism for the formation of REBCO films, which is a well-understood process and much easier to handle than the alternative fluorine-free process. A big advantage of a decreasing fluorine content in the precursor solutions is the possibility to increase the heating rate of the pyrolysis for YBCO films. In the particular case of the ELF solutions, excellent superconducting properties of YBCO films have been achieved using much faster heating rates than with other types of solutions. However, the ELF solutions have not been investigated for the synthesis of other REBCO compounds apart from our recent work on SmBCO films [12]. Here, we extend those investigations on ELF REBCO films towards mixed RE films, especially $Yb_{1-x}Sm_xBa_2Cu_3O_{7-\delta}$ (YbSmBCO) containing RE ions with very small (Yb) and very large (Sm) diameter.

2. Experimental procedure

2.1. Solution and thin film preparation

The YbSmBCO-ELF solutions were prepared following the procedure explained in detail in [12]: Yb, Sm and Cu acetates (purity > 99.99%, Alfa Aesar) were dissolved in the desired stoichiometry in propionic acid (99%). Concerning Ba, 1/3 of the Ba acetate was dissolved in trifluoroacetic acid and deionized water to convert it to TFA while the remaining 2/3 were also dissolved in propionic acid together with the other acetates. Afterwards, the two solutions were dried in a rotary evaporator, and the resulting highly viscous residues were re-diluted in anhydrous methanol (99.9%). After an iterative purification process, both solutions were mixed, and the final concentration of 2 mol l^{-1} (sum of total metal concentration) was adjusted by adding or evaporating methanol. With this procedure, an F/Ba ratio of 2 was achieved, which is the minimum amount of F necessary to allow a full conversion of the Ba precursor to BaF_2 avoiding the detrimental BaCO_3 formation [29].

The final solutions with different Yb/Sm compositions were deposited on (100)-oriented LaAlO_3 (LAO) single crystal substrates via spin coating (6000 r.p.m., 2 min). The as-deposited films were pyrolysed and grown with the thermal profiles and gas mixture given in [12]: heating with $20^\circ\text{C min}^{-1}$ in a flow of 2 l min^{-1} of pure O_2 for the pyrolysis at 500°C , and heating with $20^\circ\text{C min}^{-1}$ in 2 l min^{-1} of an N_2/O_2 mixture with 50–200 ppm O_2 for the growth at $720\text{--}820^\circ\text{C}$. The pyrolysis parameters were the same for all solutions while crystallization temperature, T_{cryst} , and oxygen partial pressure, $p\text{O}_2$, had to be adjusted in the given ranges for each composition.

2.2. Thin film characterization

The critical temperature T_c ($T_{c,90}$, i.e. the temperature of 90% normal state resistance above the transition), ΔT_c ($T_{c,90} - T_{c,10}$), $J_c(B)$ (via voltage-current $V(I)$ curves with $1 \mu\text{V cm}^{-1}$ criterion) and pinning force density $F_p = J_c \cdot B$ of the films were studied via transport measurements in four-point geometry on a 14 T Quantum Design physical property measurement system (PPMS). The measurements were done on 10–20 μm wide tracks prepared by photolithography and wet-chemical etching. The dimensions of the tracks were determined by a Bruker Dimension Edge atomic force microscope (AFM). The average thickness of all films in this work was approximately 270 nm.

3. Results and discussion

3.1. Growth process of $\text{Yb}_{1-x}\text{Sm}_x\text{Ba}_2\text{Cu}_3\text{O}_{7-\delta}$ films

The pyrolysis with a heating rate of $20^\circ\text{C min}^{-1}$ led to homogeneous, smooth and defect-free films confirming the results of [12]. As reported in [21], the crystallization temperature, T_{cryst} , and the oxygen partial pressure, $p\text{O}_2$, need to be adjusted for each composition since they depend strongly on the RE ion size. This optimization for each Sm content x was carried out following the strategy of [21]: varying T_{cryst} and $p\text{O}_2$ independently by keeping the respective other parameter constant while searching for the highest possible J_c^{sf} at 77 K and so determining iteratively the most suitable combination of T_{cryst} and $p\text{O}_2$ for each compound. Figure 1 shows the dependency of J_c^{sf} at 77 K on T_{cryst} for a constant, optimal $p\text{O}_2$ for each composition. The optimal T_{cryst} of the pure YbBCO (approx. 720°C) and SmBCO (approx. 810°C) films differ by 90°C due to the large difference in RE ion size. The optimal T_{cryst} for the mixed compounds was searched for by exploring the temperature range spanned by the pure phases. While the maxima lie between the optima of the pure phases as expected, the mixed compounds surprisingly show a narrower T_{cryst} range for reasonable J_c^{sf} values at 77 K than the single-phase compounds. This suggests that the formation of mixed REBCO compounds with very different RE ion sizes is rather complex and requires specific growth conditions to reach reasonable superconducting properties. This is strikingly different to our recent work on full-TFA grown mixed RE films with RE sizes not too far apart [23], which presented smoother and even wider temperature windows than the single-phase compounds. The optimal $p\text{O}_2$ values follow the same trend as the ones reported in [21] with lower values for the compounds with bigger RE^{3+} ion size, i.e. for larger x values. Table 1 summarizes the most suitable parameters T_{cryst} and $p\text{O}_2$ for the Sm contents x in our study as well as the resulting physical properties.

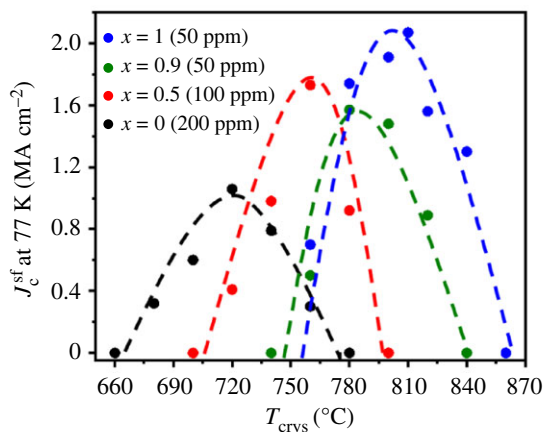


Figure 1. Dependence of J_c^{sf} at 77 K on T_{crys} for $Yb_{1-x}Sm_xBa_2Cu_3O_{7-\delta}$ films with $x = 0, 0.5, 0.9$ and 1 at their optimal pO_2 value. The dashed lines are guides for the eyes.

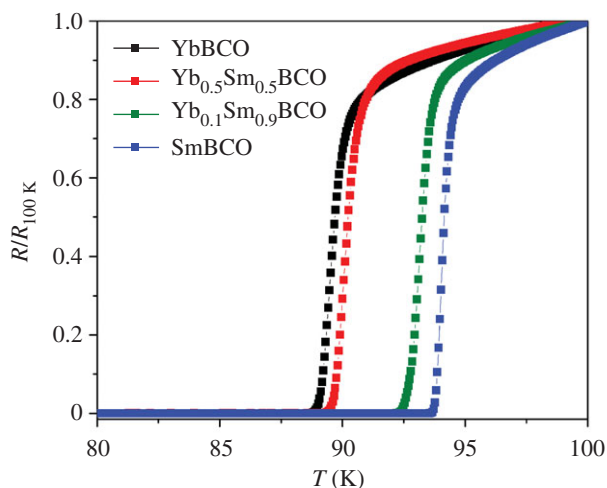


Figure 2. Normalized $R(T)$ curves of $Yb_{1-x}Sm_xBa_2Cu_3O_{7-\delta}$ films grown with the parameters in table 1.

Table 1. Optimal crystallization temperature (T_{crys}) and oxygen partial pressure (pO_2) for the growth of $Yb_{1-x}Sm_xBa_2Cu_3O_{7-\delta}$ films and the superconducting properties of films grown at these conditions.

x	T_{crys} (°C)	pO_2 (ppm)	T_c (K)	ΔT (K)	J_c^{sf} 77 K (MA cm ⁻²)	J_c^{sf} 65 K (MA cm ⁻²)	J_c^{sf} 30 K (MA cm ⁻²)	H^* 77 K (mT)	H^* 65 K (mT)	H^* 30 K (mT)
0	720	200	90.5	1.1	1.1	2.0	3.9	8	17	29
0.5	760	100	91.1	1.3	1.7	2.9	4.8	13	32	44
0.9	780	50	93.9	1	1.6	2.9	6.1	10	47	56
1	810	50	95.0	0.9	2.1	3.0	4.7	11	20	34

3.2. Superconducting properties of $Yb_{1-x}Sm_xBa_2Cu_3O_{7-\delta}$ films

The Yb-containing films present similar microstructural characteristics to the SmBCO films in [12]: a strong preference for the c -axis orientation together with occasionally surfacing misoriented grains. This has been the first time that ELF solutions were used to successfully grow this type of films, and one of the first to study this RE combination at all [33].

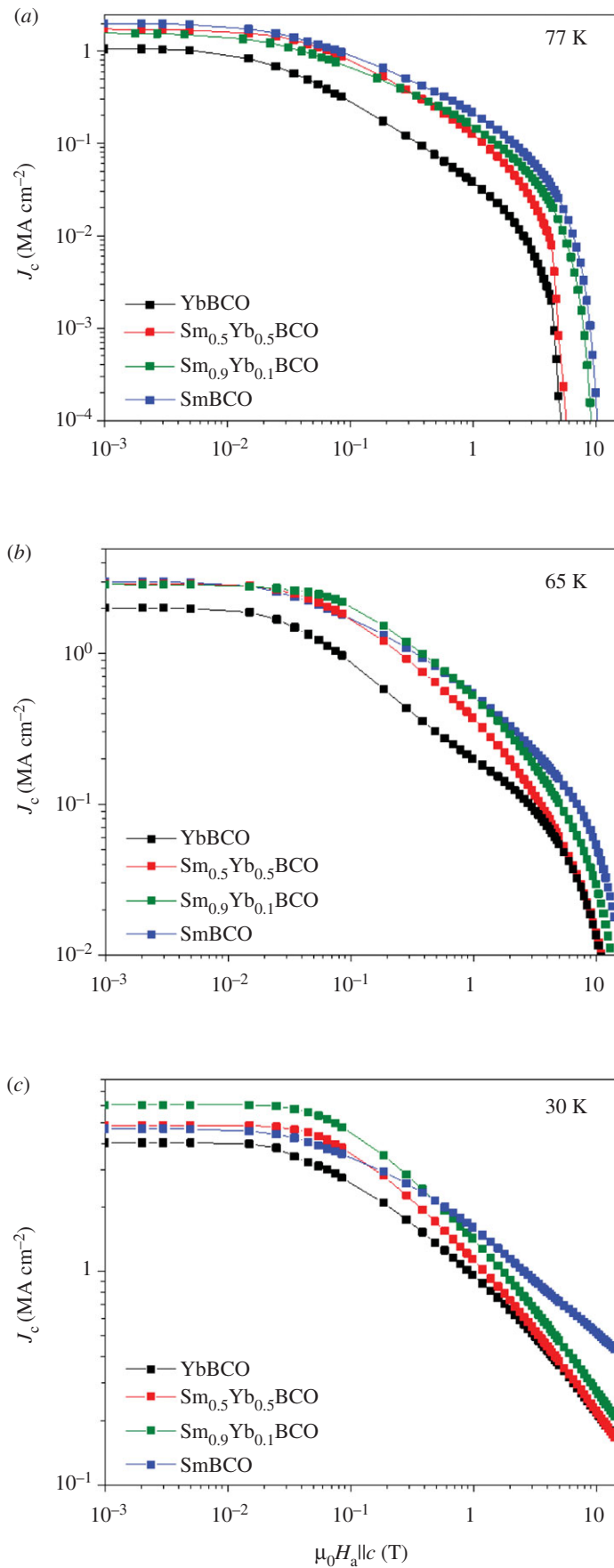


Figure 3. J_c dependence on magnetic field of $\text{Yb}_{1-x}\text{Sm}_x\text{Ba}_2\text{Cu}_3\text{O}_{7-\delta}$ films at (a) 77, (b) 65 and (c) 30 K.

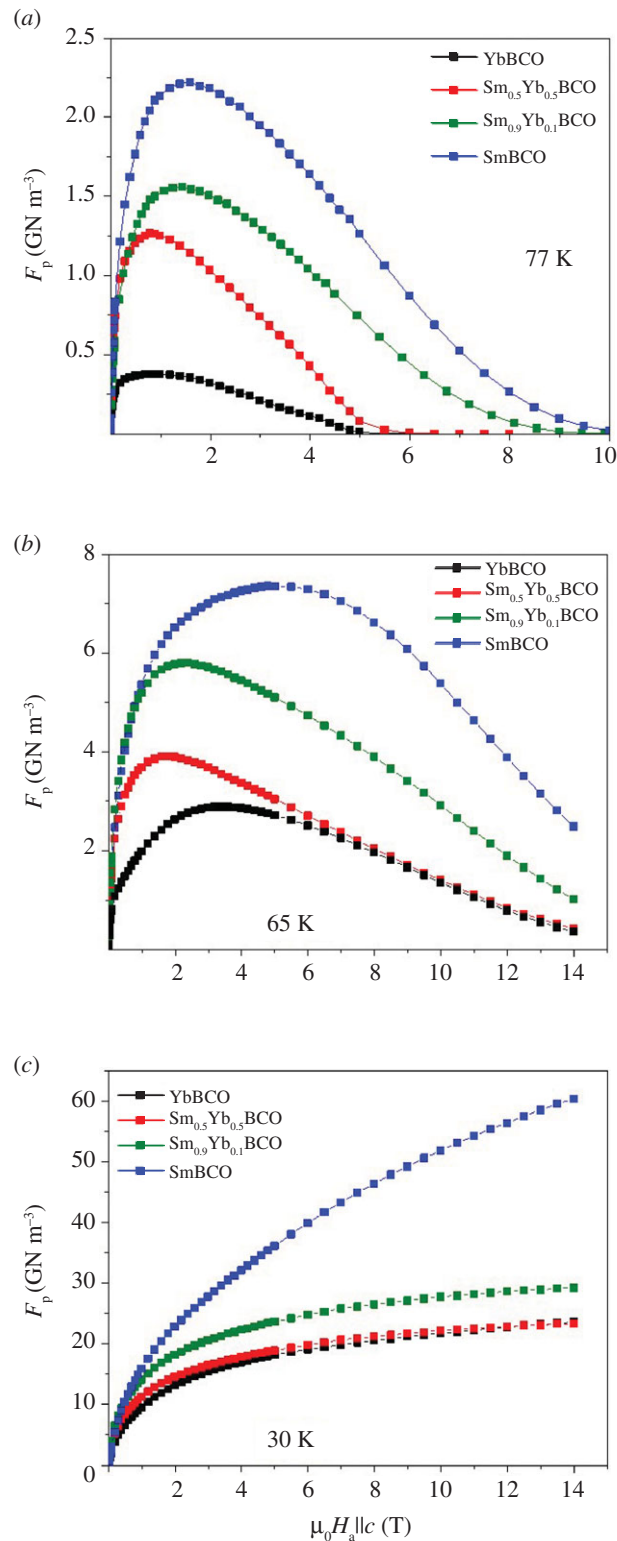


Figure 4. F_p dependence on magnetic field of $\text{Yb}_{1-x}\text{Sm}_x\text{Ba}_2\text{Cu}_3\text{O}_{7-\delta}$ films at (a) 77, (b) 65 and (c) 30 K.

The T_c values, figure 2, vary between approximately 90.5 K for the pure YbBCO films and approximately 95 K for the pure SmBCO films. These values are similar to the ones reported in previous works for YbBCO [13–18] and SmBCO films [12,34–36] prepared by different techniques and also resemble previously reported values for YbSmBCO bulk samples [33]. The influence of Yb content on T_c is very remarkable. Already 10% of Yb ($x=0.9$) reduces T_c by approximately 1 K. Moreover, for $x=0.5$, the T_c of approximately 91 K is very similar to the pure YbBCO value. Thus, T_c is not following a linear dependence as reported in, for example, [13] for the case of

$\text{Y}_{1-x}\text{Gd}_x\text{Ba}_2\text{Cu}_3\text{O}_{7-\delta}$ films. The films with $x = 0.5$ have the largest ΔT_c of approximately 1.3 K, while in the rest of the films ΔT_c is approximately 1 K.

The magnetic field dependences of J_c at three different temperatures are compared in figure 3. J_c^{sf} at 77 K varies between approximately 1 MA cm^{-2} for pure YbBCO and approximately 2 MA cm^{-2} for pure SmBCO with the films with $x = 0.5$ and $x = 0.9$ in between. Although these values seem to be quite modest, they are among the largest published for YbBCO [13–18] and also SmBCO films [12,34–36] grown by different techniques. However, at lower temperatures, the mixed films start to compete with the pure phases. At 65 K, J_c^{sf} increases to the range approximately 3 MA cm^{-2} for the Sm-containing films and approximately 2 MA cm^{-2} for the pure YbBCO film. At 30 K, the film with $x = 0.9$ presents the largest J_c^{sf} of approximately 6 MA cm^{-2} followed by the two other Sm-containing samples with J_c^{sf} approximately 5 MA cm^{-2} and, again, the pure YbBCO film has the lowest value of approximately 4 MA cm^{-2} . This behaviour is a combined effect of T_c , microstructural defects and additional pinning due to RE mixing. The fact that at low temperatures, the mixed films have larger J_c^{sf} does, however, not mean that the in-field values are higher. At 65 and 30 K, the mixed films show larger J_c values at low fields but smaller values than SmBCO above a certain cross-over magnetic field. This cross-over depends both on x and temperature and is related to the fact that the values of the exponent α ($J_c \sim B^{-\alpha}$) are larger for the mixed films or in other words to opposing trends for J_c^{sf} and irreversibility field (H_{irr}). The same behaviour of mixed films with different combinations of RE ions was observed by MacManus-Driscoll *et al.* at 77 K [19]. In that work, this effect of enhancing the pinning at low fields was attributed to the random point-like disorder in those films, namely random displacements of oxygen ions due to the ion size variance. This could also be the explanation for the behaviour observed in our films.

Figure 4 displays the magnetic field dependence of the pinning force density (F_p) of the YbSmBCO films. The largest absolute F_p values belong to the pure SmBCO film at all temperatures: approximately 2.2 (at 1.6 T), approximately 7.4 (at 5.1 T) and greater than 60 GN m^{-3} at 77, 65 and 30 K, respectively. Due to the larger accommodation field H^* , defined as $J_c(H^*) = 0.9 J_c^{\text{sf}}$, there are narrow low-field regions at 65 and 30 K where J_c and hence F_p of the mixed films is larger. However, the maximum values of these films are lower than for the SmBCO film, e.g. approximately 1.5 (at 1.4 T), approximately 5.7 (at 2.3 T) and approximately 29.3 GN m^{-3} at 77 K, 65 K and 30 K, respectively, for $x = 0.9$.

4. Conclusion

The main objective of this work was to study the superconducting properties of REBCO films with a mixture of RE ions with large difference in ion size, in particular Sm^{3+} and Yb^{3+} . Despite the challenges associated with the ion size itself (Ba^{2+} substitution with Sm^{3+} and ion vacancies with Yb^{3+}) and with the large difference in the optimum crystallization temperature between both pure compounds, it was possible to synthesize superconducting $\text{Yb}_{1-x}\text{Sm}_x\text{Ba}_2\text{Cu}_3\text{O}_{7-\delta}$ (YbSmBCO) films on LAO substrates by CSD using ELF solutions. The T_c values are largely influenced by the presence of Yb^{3+} ions. The J_c values at low fields, especially at low temperatures, increase by the use of mixed phases but are inferior to values of pure compounds at high fields.

Ethics. Our investigation was carried out in full accordance with the ethical guidelines of our research institution.

Data accessibility. Data supporting this study are available from the Dryad Digital Repository: <https://doi.org/10.5061/dryad.jsxksn06p> [37].

Authors' contributions. P.C. and M.L. carried out the preparation of the films and the data analysis and wrote the manuscript. M.E., Z.L., C.C., J.H. and B.H. supervised the work. All authors discussed the results and contributed to the manuscript.

Competing interests. We declare we have no competing interests.

Funding. This work was supported in part by the Science and Technology Commission of Shanghai Municipality (grant nos. 16521108402, 13111102300 and 14521102800), the National Natural Science Foundation of China (grant no. 51572165) and National Key Research and Development Program (grant no. 2016YFF0101701).

Acknowledgements. We acknowledge support by the KIT Publication Fund of the Karlsruhe Institute of Technology.

References

1. Larbalestier D, Gurevich A, Feldmann DM, Polyanski A. 2001 High- T_c superconducting materials for electric power applications. *Nature* **414**, 368–377. (doi:10.1038/35104654)
2. Shiohara Y, Taneda T, Yoshizumi M. 2012 Overview of materials and power applications of

- coated conductors project. *Jpn. J. Appl. Phys.* **51**, 010007. (doi:10.1143/JJAP.51.010007)
3. Obradors X, Puig T. 2014 Coated conductors for power applications: materials challenges. *Supercond. Sci. Technol.* **27**, 044003. (doi:10.1088/0953-2048/27/4/044003)
 4. Murakami M, Sakai N, Higuchi T, Yoo SI. 1996 Melt-processed light rare earth element—Ba—Cu—O. *Supercond. Sci. Technol.* **9**, 1015–1032. (doi:10.1088/0953-2048/9/12/001)
 5. Yoshida Y, Matsumoto K, Miura M, Ichino Y, Takai Y, Ichinose A, Horii S, Mukaida M. 2005 High-critical-current-density epitaxial films of $\text{SmBa}_2\text{Cu}_3\text{O}_{7-x}$ in high fields. *Jpn. J. Appl. Phys. Part 2 Lett.* **44**, L129–L132.
 6. Yoshida T, Ibi A, Takahashi T, Yoshizumi M, Izumi T, Shiohara Y. 2014 Fabrication of $\text{Eu}_1\text{Ba}_2\text{Cu}_3\text{O}_{7-\delta}+\text{BaHfO}_3$ coated conductors with 141 A/cm-w under 3 T at 77 K using the IBAD/PLD process. *Phys. C Supercond. Appl.* **504**, 42–46. (doi:10.1016/j.physc.2014.03.013)
 7. Cayado P, Erbe M, Kauffmann-Weiss S, Bühler C, Jung A, Hänisch J, Holzapfel B. 2017 Large critical current densities and pinning forces in CSD-grown superconducting $\text{GdBa}_2\text{Cu}_3\text{O}_{7-x}-\text{BaHfO}_3$ nanocomposite films. *Supercond. Sci. Technol.* **30**. (doi:10.1088/1361-6668/aa7e47)
 8. Miura S, Tsuchiya Y, Yoshida Y, Ichino Y, Awaji S, Matsumoto K, Ibi A, Izumi T. 2017 Strong flux pinning at 4.2 K in $\text{SmBa}_2\text{Cu}_3\text{O}_y$ coated conductors with BaHfO_3 nanorods controlled by low growth temperature. *Supercond. Sci. Technol.* **30**, 084009. (doi:10.1088/1361-6668/aa76a1)
 9. Islam MS, Baetzold RC. 1989 Atomistic simulation of dopant substitution in $\text{YBa}_2\text{Cu}_3\text{O}_7$. *Phys. Rev. B* **40**, 10 926–10 935. (doi:10.1103/PhysRevB.40.10926)
 10. Andreouli C, Tsetsekou A. 1997 Synthesis of HTSC $\text{Re}(\text{Y})\text{Ba}_2\text{Cu}_3\text{O}_x$ powders: the role of ionic radius. *Phys. C Supercond.* **291**, 274–286. (doi:10.1016/S0921-4534(97)01636-5)
 11. MacManus-Driscoll JL. 1997 Materials chemistry and thermodynamics of $\text{REBa}_2\text{Cu}_3\text{O}_{7-x}$. *Adv. Mater.* **9**, 457–473. (doi:10.1002/adma.19970090602)
 12. Li M, Erbe M, Jung A, Hänisch J, Holzapfel B, Liu Z, Cai C. 2020 Rapid pyrolysis of $\text{SmBa}_2\text{Cu}_3\text{O}_{7-\delta}$ films in CSD-MOD using extremely-low-fluorine solutions. *Coatings* **10**, 31. (doi:10.3390/coatings10010031)
 13. Ma XL, Yamagiwa K, Shibata J, Hirayama T, Hirabayashi I, Ikuhara Y. 1999 Characterization of the $\text{YbBa}_2\text{Cu}_3\text{O}_{7-y}$ and $\text{YBa}_2\text{Cu}_3\text{O}_{7-y}$ thin superconducting films prepared by chemical solution deposition on $\text{MgO}(001)$ substrate. *J. Electron Microsc.* **48**, 785–789. (doi:10.1093/oxfordjournals.jmicro.a023749)
 14. Ma XL, Shibata J, Hirayama T, Yamagiwa K, Hirabayashi I, Ikuhara Y. 1999 Characterization of $\text{YbBa}_2\text{Cu}_3\text{O}_{7-y}$ superconducting thin films prepared by chemical solution deposition on $\text{SrTiO}_3(001)$ and $\text{LaAlO}_3(001)$ substrates. *Phys. Status Solidi* **173**, 441–450. (doi:10.1002/(SICI)1521-396X(199906)173:2<441::AID-PSSA441>3.0.CO;2-Y)
 15. El-Kawni MI, Okuyucu H, Aslanoglu Z, Akin Y, Hascicek YS. 2003 Growth and characterization of YbBCO films on textured Gd_2O_3 buffer-layered Ni tapes: all sol–gel process. *J. Supercond.* **16**, 533–536. (doi:10.1023/A:1023877222308)
 16. Matsubara I, Paranthaman M, Chirayil TG, Sun EY, Martin M, Kroeger DM, Verebelyi DT, Christen DK. 1999 Preparation of epitaxial $\text{YbBa}_2\text{Cu}_3\text{O}_{7-\delta}$ on SrTiO_3 single crystal substrates using a solution process. *Jpn. J. Appl. Phys. Part 2 Lett.* **38**, L727. (doi:10.1143/JJAP.38.L727)
 17. Ishiura H, Tsuji N, Mori H, Nohira H. 1992 Preparation of $\text{YbBa}_2\text{Cu}_3\text{O}_{7-x}$ films on $\text{Si}(100)$ substrates using SrTiO_3 buffer layers. *Appl. Phys. Lett.* **61**, 1459–1461. (doi:10.1063/1.107517)
 18. Shibata J, Yamagiwa K, Hirabayashi I, Hirayama T, Ikuhara Y. 2000 Transmission electron microscopic studies of $\text{YbBa}_2\text{Cu}_3\text{O}_{7-\delta}$ superconducting final films formed on $\text{LaAlO}_3(001)$ substrates by the dipping-pyrolysis process. *Jpn. J. Appl. Phys., Part 1 Regul. Pap. Short Notes Rev. Pap.* **39**, 3361–3365. (doi:10.1143/JJAP.39.3361)
 19. MacManus-Driscoll JL et al. 2004 Systematic enhancement of in-field critical current density with rare-earth ion size variance in superconducting rare-earth barium cuprate films. *Appl. Phys. Lett.* **84**. (doi:10.1063/1.1766394)
 20. MacManus-Driscoll JL et al. 2005 Rare earth ion size effects and enhanced critical current densities in $\text{Y}_{2/3}\text{Sm}_{1/3}\text{Ba}_2\text{Cu}_3\text{O}_{7-x}$ coated conductors. *Appl. Phys. Lett.* **86**, 032505. (doi:10.1063/1.1851006)
 21. Cayado P, Erbe M, Kauffmann-Weiss S, Jung A, Hänisch J, Holzapfel B. 2018 Chemical solution deposition of $\text{Y}_{1-x}\text{Gd}_x\text{Ba}_2\text{Cu}_3\text{O}_{7-\delta}-\text{BaHfO}_3$ nanocomposite films: combined influence of nanoparticles and rare-earth mixing on growth conditions and transport properties. *RSC Adv.* **8**, 42 398–42 404. (doi:10.1039/C8RA09188A)
 22. Nelstrop JA, MacManus-Driscoll J. 2002 Phase stability of erbium barium cuprate, $\text{ErBa}_2\text{Cu}_3\text{O}_{7-x}$ and ytterbium barium cuprate, $\text{YbBa}_2\text{Cu}_3\text{O}_{7-x}$. *Phys. C Supercond.* **377**, 585–594. (doi:10.1016/S0921-4534(02)00630-5)
 23. Jia QX, Foltyn SR, Arendt N, Wang H, MacManus-Driscoll JL, Coulter Y, Li Y, Maley MP, Hawley M. 2003 The role of a superconducting seed layer in the structural and transport properties of $\text{EuBa}_2\text{Cu}_3\text{O}_{7-x}$ films. *Appl. Phys. Lett.* **83**, 1388–1390. (doi:10.1063/1.1601680)
 24. Gupta A, Jagannathan R, Cooper EI, Giess EA, Landman JI, Hussey BW. 1988 Superconducting oxide films with high transition temperature prepared from metal trifluoroacetate precursors. *Appl. Phys. Lett.* **52**, 2077–2079. (doi:10.1063/1.99752)
 25. Arvanitidis I, Sichen D, Seetharaman S. 1996 A study of the thermal decomposition of BaCO_3 . *Metall. Mater. Trans. B* **27**, 409–416. (doi:10.1007/BF02914905)
 26. Chen H, Zalamosa K, Pomar A, Granados X, Puig T, Obradors X. 2010 Growth rate control and solid–gas modeling of $\text{TFA-YBa}_2\text{Cu}_3\text{O}_7$ thin film processing. *Supercond. Sci. Technol.* **23**, 034005. (doi:10.1088/0953-2048/23/3/034005)
 27. Obradors X et al. 2006 Progress towards all-chemical superconducting $\text{YBa}_2\text{Cu}_3\text{O}_7$ -coated conductors. *Supercond. Sci. Technol.* **19**, S13–S26. (doi:10.1088/0953-2048/19/3/003)
 28. Erbe M, Hänisch J, Freudenberg T, Kirchner A, Mönch I, Kaskel S, Schultz L, Holzapfel B. 2014 Improved $\text{REBa}_2\text{Cu}_3\text{O}_{7-x}$ ($\text{RE}=\text{Y, Gd}$) structure and superconducting properties by addition of acetylacetone in TFA-MOD precursor solutions. *J. Mater. Chem. A* **2**, 4932. (doi:10.1039/c3ta15243j)
 29. Wu W et al. 2014 A low-fluorine solution with a 2:1 F/Ba mole ratio for the fabrication of YBCO films. *Supercond. Sci. Technol.* **27**, 055006. (doi:10.1088/0953-2048/27/5/055006)
 30. Palmer X et al. 2016 Solution design for low-fluorine trifluoroacetate route to $\text{YBa}_2\text{Cu}_3\text{O}_7$ films. *Supercond. Sci. Technol.* **29**, 024002. (doi:10.1088/0953-2048/29/2/024002)
 31. Cayado P et al. 2017 Epitaxial superconducting $\text{GdBa}_2\text{Cu}_3\text{O}_{7-\delta}-\text{Gd}_2\text{O}_3$ nanocomposite thin films from advanced low-fluorine solutions. *Supercond. Sci. Technol.* **30**, 125010. (doi:10.1088/1361-6668/aa8ffe)
 32. Li M, Yang W, Shu G, Bai C, Lu Y, Guo Y, Liu Z, Cai C. 2015 Controlled-growth of film using modified low-fluorine chemical solution deposition. *IEEE Trans. Appl. Supercond.* **25**, 6601804.
 33. Taguchi I. 1988 Effect of lattice distortions on 90-K class superconductors: $\text{Y}_{1-x}\text{Eu}_x\text{Ba}_2\text{Cu}_3\text{O}_{7-\delta}$, $\text{Yb}_{1-x}\text{Sm}_x\text{Ba}_2\text{Cu}_3\text{O}_{7-\delta}$ and $\text{Eu}(\text{Ba}_{1-x}\text{Sr}_x)_2\text{Cu}_3\text{O}_{7-\delta}$. *Jpn. J. Appl. Phys.* **27**, 1058–1060. (doi:10.1143/JJAP.27.L1058)
 34. Fuger R, Eisterer M, Oh SS, Weber HW. 2010 Superior properties of SmBCO coated conductors at high magnetic fields and elevated temperatures. *Phys. C Supercond. Appl.* **470**, 323–325. (doi:10.1016/j.physc.2010.01.060)
 35. Mitani A et al. 2008 Effect of fabrication conditions on crystalline of SmBCO films fabricated by TFA-MOD method. *Physica C* **468**, 1546–1549. (doi:10.1016/j.physc.2008.05.066)
 36. Wang Z, Wang WT, Yang XF, Wang MJ, Zhao Y. 2014 Preparation of high-performance $\text{SmBa}_2\text{Cu}_3\text{O}_{7-x}$ superconducting films by chemical solution deposition approach. *J. Supercond. Nov. Magn.* **27**, 1801–1806. (doi:10.1007/s10948-014-2523-2)
 37. Cayado P, Li M, Erbe M, Liu Z, Cai C, Hänisch J, Holzapfel B. 2020 Data from: REBCO mixtures with large difference in rare-earth ion size: superconducting properties of chemical solution deposition-grown $\text{Yb}_{1-x}\text{Sm}_x\text{Ba}_2\text{Cu}_3\text{O}_{7-\delta}$. Dryad Digital Repository. (doi:10.5061/dryad.jsxksn06p)